Hindawi
Advances in Civil Engineering
Volume 2020, Article ID 8843172, 10 pages
https://doi.org/10.1155/2020/8843172

Research Article

Experimental and Theoretical Investigation of Overburden Failure Law of Fully Mechanized Work Face in Steep Coal Seam

Ze Liao[1], **Tao Feng**[1], **Weijian Yu**[1], **Genshui Wu**[2] **and Ke Li**[1,3]

[1]*School of Resource & Environment and Safety Engineering, Hunan University of Science and Technology, Xiangtan, Hunan 411201, China*
[2]*School of Mechanics and Civil Engineering, China University of Mining & Technology, Beijing, Xuzhou 100083, China*
[3]*College of Mining, Guizhou Institute of Technology, Guiyang, Guizhou 550003, China*

Correspondence should be addressed to Weijian Yu; ywjlah@163.com

Received 27 June 2020; Revised 1 September 2020; Accepted 16 September 2020; Published 28 September 2020

Academic Editor: Fengqiang Gong

In this study, both theoretical analysis and similar simulation experiment are employed to investigate the overburden failure law of fully mechanized face in the steep coal seam. By establishing the mechanical model of inclined rock beam, the deflection equation of overlying strata beam is obtained. Based on the geological conditions of Xiangyong coal mine in Hunan Province of China, the laws of roof deformation and failure in steep coal seam are obtained by similar simulation experiments. The results showed that the roof deformation of the goaf is relatively large after the working face advances along the strike, and the deformation mainly occurs in the upper roof of the goaf. The backward gangue in the immediate roof fills the lower part of the goaf, which plays a supporting role in the lower part of the roof and floor. The roof fracture of goaf is located in the middle and upper parts of the working face, which is consistent with the results derived from the mechanical model. After the roof fracture, a "trapezoid" bending fracture area and the secondary stability system area is formed, which is composed of four areas: the lower falling and filling support area, the upper strata bending fracture area, the fracture extension area, and the roof bending sinking area.

1. Introduction

The reserves of large dip or steeply inclined coal seams account for about 10–20% of the total coal reserves in China [1, 2]. The main characteristics of surrounding rock movement and deformation after mining in steep coal seam are different from that in gently inclined or near horizontal coal seam [3–5]. The movement law of overlying strata, especially, is quite different from that in the gently inclined coal seam. In recent years, many mining areas began to pay attention to thin seam mining and did the corresponding basic research work with the increase of mining intensity and the rapid depletion of high-quality coal resources [6–8]. Many mining areas have to consider the steep coal seam mining in order to ensure the sustainable development of the mine. Due to the lack of relevant theoretical support such as overburden movement law and reasonable mining method in steep coal seam mining, the surrounding rock control of steep coal seam working face is difficult, the safety condition is poor, and the speed of promotion is slow, which lead to the frequent occurrence of mine dynamic disasters [9–11]. Therefore, many experts and scholars have done much research with basic theory and engineering practice on many vital problems and difficulties in the mining of steep coal seam. Wu [12] put forward the "R-S-F" system dynamics control theory and laid the theoretical and technical foundation for the mining of steep coal seam. Yang [13] analyzed the stability of overburden "factory" type mobile arch slab in steeply inclined coal seam by using the theory of thin plate under small deflection and analyzed the deformation failure mechanism and influencing factors of steeply inclined soft-hard interbedded roadway. Zhang et al. [14] analyzed the stress distribution characteristics and breaking mechanism of the basic roof break on up-dip or down-dip mining stope at a deep angle by using the thin plate mechanical model. Tu [15–17] studied the filling and compaction characteristics of

gangue in the steeply inclined working face and revealed that the immediate roof is in the shape of an "ear" bearing shell, and the main roof is broken by the inclined "voussoir beam" structure. Yin et al. [18, 19] established a mechanical model of overburden deformation of coal seam with large dip angle and found that the maximum deflection point of the simply supported inclined thin plate on four sides is located at the lower part of the middle in the goaf. Xie et al. [20–22] simplified the basic roof as the statically indeterminate beam model and analyzed the movement law and ladder type failure structure of the stope roof in the coal seam with large dip angle and large mining height. Based on stress arch theory, Wang et al. [23] proposed the evolution discriminant coefficient for determining the evolution characteristics of stress arch in overburden rock and analyzed the movement law of stress arch shell. Yao et al. [24, 25] established the mechanical model of inclined strata in the steep seam fully mechanized mining with sublevel filling along the strike by using the theory of small deflection of the thin elastic plate. Based on different theories and engineering backgrounds, scholars have different research results on the mining of steep coal seam, which shows that the deformation and fracture of the roof in the mining of steep coal seam are very complicated, such as nonuniformity and asymmetry [26–28]. It is necessary to explore further the failure law of overburden in the fully mechanized mining face of the steep coal seam.

Based on the engineering geological data of #6 coal seam in Xiangyong coal mine, Hunan Province, China, both theoretical analysis and similar simulation experiment are employed to obtain the failure characteristics and strata movement law of fully mechanized mining face in the steep coal seam, which provides a theoretical reference for the control of mining pressure in the steep coal seam.

2. Mining Characteristics of Steep Coal Seam

Due to the unbalanced subsidence of the earth's crust, the magmatic erosion, the result of the movement breaking and folding in the original geological structure and the geological conditions of the steep coal seam were diversified. At the same time, the more complex the geological structure movement is, the greater the change of the coal seam dip angle is, and the higher the degree of coal metamorphism is. Most of the steeply inclined coal seams in China are mainly in multiseam occurrence mode and have a large thickness variation. Under the influence of geological structure movement after coal formation, the coal seam morphology is more complicated, and even the same coal seam may undergo large thickness variations.

The large inclination of the steeply inclined coal seam allows coal and gangue to slide down automatically, which can greatly reduce the coal transportation workload and help to cut coal downward, but at the same time, it will pose a personal threat to the equipment personnel at the working face. With the development of joints in the steep coal seam and surrounding rock, the first weighting and periodic weighting of the roof are not very obvious, and it is easy to occur spontaneous roof collapse without signs. At the same time, the component force of the roof pressure exerted on the coal pillars or supported along the vertical direction of the coal seam is much smaller than the pressure exerted on the roof of the gently inclined coal seam, and the component force acting along the inclined direction of the coal seam is larger, so the support of the working face is prone to topple and slide, making the supporting work more complicated and difficult [29]. The mining of steeply inclined with close-distance coal seam groups has a great influence on each other. When the dip angle of the coal seam is larger than the moving angle of the roof rock and the floor rock, the roof and floor of the coal seam may move or even slide after mining. It is very likely to damage the integrity of the roof and floor of the coal seam that has not been mined in the upper and lower part, and it is unfavourable to the mining of the adjacent coal seam [30, 31].

The stability of the roof rock layer was reduced after the steep coal seam had been mined, and the overlying strata of coal seam would bend and deform in the normal direction under the action of gravity. At the same time, the rock mass after breaking and falling will slide and move towards the lower part of the goaf along the direction of the working face inclination due to the force component along the normal inclined direction of the bedding plane. The rock of the coal seam floor will also slide down when the dip angle of the coal seam exceeds 50°. Because the gravity direction of the rock is not perpendicular to the bedding plane, the component force of the rock gravity along the bedding plane will make the roof and floor rock easily move downward along the bedding plane. The larger the dip angle of the steep coal seam is, the stronger the sliding of the roof and floor is.

3. Mechanical Model of Overburden Movement in Steep Coal Seam

3.1. Establishment of Mechanical Model. With the increase of coal seam dip angle, the gravity of the roof increases along with the coal seam layer, which promotes the downward sliding trend of the roof. As the steeply inclined working face advances along the direction, the lower part of the mined-out area is directly supported by the gangue falling to support the lower roof, while the upper part of the mined-out area has a large area of roof overhang with the coal seam is mined. The basic roof will be bending deformation or even broken under the action of gravity and overburden pressure.

The mechanical model of goaf roof after steep seam mining was established, and its basic roof was simplified as the mechanical model of inclined rock beam. The collapsed gangue automatically slides to the lower part of the goaf to support and restrict the roof after the steep coal seam has been mined. Therefore, the deformation of the lower part of the working face roof is small, which can be simplified as the fixed support ends. The upper part of the working face roof can be simplified as the simple support ends due to the impact of the roof rock mass breaking, caving, sliding, and so on. The stress analysis diagram of the roof is shown in Figure 1.

In Figure 1, P is the axial force of the overlying strata on the inclined strata, $q0$ is the component force of the gravity

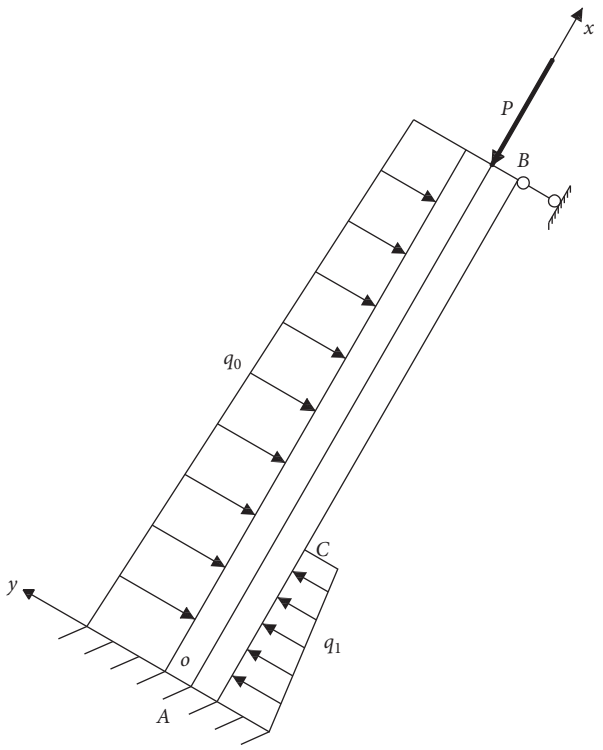

Figure 1: Stress analysis of the roof in steep coal seam.

of the overlying strata on the vertical strata level, and $q1$ represents the filling reaction force of the collapsed gangue sliding and filling body in the direction perpendicular to the strata level. The dip angle of the coal seam is 60°, A is the fixed support ends, B is the simple support ends, and C is the filling range of gangue falling across. The self-weight of rock beam is ignored since the self-weight of the roof is small relative to the whole in situ stress. With the degree of compaction from lower to top, the reaction force of the lower natural falling gangue filling gradually becomes zero, and $q1$ can be expressed as follows:

$$q_1 = F_0\left(1 - \frac{x}{l}\right), \quad (0 \le x \le l), \tag{1}$$

where F_0 is the maximum value of the lower filling reaction force, and l is the filling length of the gangue in the lower part of the goaf. The maximum filling reaction force F_0 and the lower gangue cross-filling length l were determined by the gangue filling body and the expansion of the rock; when H_1 is the buried depth of the upper boundary in the working face, H_2 is the buried depth of the lower boundary, and l is the length of the working face, the filling reaction can be expressed as $F_0 = \gamma H_2 \cos\alpha$, the gravity of overlying strata can be expressed as $q_0 = (1/2)\gamma(H_1 + H_2)\cos\alpha$, and the axial gravity of the inclined rock beam can be expressed as $P = \gamma H_1 \sin\alpha$.

According to the roof caving and filling of the working face and the expansion of the gangue, the filling length of the gangue naturally caving and filling in the lower part of the goaf can be expressed as follows:

$$l = \frac{k_1 L(h_1 + h_2)}{M + h_1 + k_1 h_2}, \tag{2}$$

where L is the length of working face, k_1 represents the expansion coefficient of falling rock, M is the thickness of coal seam, h_1 represents the thickness of rock stratum which is easy to collapse, and h_2 is the thickness of lagging collapse.

3.2. Mechanical Analysis of Overburden Movement. According to the mechanical model in Figure 1, the support force in the normal direction of the upper boundary is R_B, and the support force in the normal direction of the lower boundary is R_A. The constraint of the support force on the roof is calculated according to the balance condition, and it can be expressed as follows:

$$\begin{aligned} R_A &= \frac{q_0 L}{2} - \frac{F_0}{2}\left(l - \frac{l}{3}\right), \\ R_B &= \frac{q_0 L}{2} - \frac{F_0 l^2}{6L}. \end{aligned} \tag{3}$$

The relationship between the load collection degree, bending moment, and shear force of rock beam is as follows:

$$\begin{aligned} \frac{dF_s(x)}{dx} &= q(x), \\ \frac{dM(x)}{dx} &= F_s(x). \end{aligned} \tag{4}$$

The shear force F_S is calculated by the load concentration $q(x)$, and then the moment of AC and BC is calculated, and it can be expressed as follows:

$$\begin{aligned} \mathrm{EI}\frac{d^2\omega}{dx^2} = M(x) &= -\frac{F_0 x^3}{6l} + \left(\frac{F_0}{2} - \frac{q_0}{2}\right)x_2 \\ &\quad + R_A x - P\omega, \ (0 \le x \le l), \\ \mathrm{EI}\frac{d^2\omega}{dx^2} = M(x) &= -\frac{q_0 x^2}{2} + \left(R_A + \frac{F_0 l}{2}\right)x \\ &\quad + \frac{F_0 l^2}{6} - P\omega, \quad (l \le x \le L), \end{aligned} \tag{5}$$

where $-P\omega$ is the influence of the axial force on the bending deformation of the rock beam. Because ω is negative, the axial force P plays a role in increasing the bending moment of rock beam. Define $k^2 = P/\mathrm{EI}$ and then

$$\begin{aligned} \frac{\mathrm{d}^2\omega}{\mathrm{d}x^2} + k^2\omega &= k^2\left[-\frac{F_0 x^3}{6Pl} + \left(\frac{F_0}{2P} - \frac{q_0}{2P}\right)x^2 + \frac{R_A x}{P}\right], \quad (0 \le x \le l), \\ \frac{\mathrm{d}^2\omega}{\mathrm{d}x^2} + k^2\omega &= k^2\left[-\frac{q_0}{2P}x^2 + \left(\frac{R_A}{P} + \frac{F_0 l}{2P}\right)x - \frac{F_0 l^2}{6P}\right], \quad (l \le x \le L). \end{aligned} \tag{6}$$

Through calculation, the general solution of the above formula is

$$\begin{aligned}\omega &= A\cos kx + B\sin kx - \frac{F_0x^3}{6Pl} + \left(\frac{F_0}{2P} - \frac{q_0}{2P}\right)x^2 \\ &\quad + \frac{R_Ax}{P} - \frac{F_0x}{Plk^2} + \frac{F_0 - q_0}{Pk^2}, \quad (0 \le x \le l), \\ \omega &= C\cos kx + D\sin kx - \frac{q_0}{2P}x^2 + \left(\frac{R_A}{P} + \frac{F_0l}{2P}\right)x \\ &\quad - \frac{F_0l^2}{6P} + \frac{q_0}{Pk^2}, \quad (l \le x \le L).\end{aligned} \tag{7}$$

Since the deflections at the ends A and B of the rock beam are zero, we can obtain the following:

$$A = \frac{F_0 - q_0}{Pk^2},$$

$$C\cos kL + D\sin kL = \frac{q_0}{2P}L^2 - \left(\frac{R_A}{P} + \frac{F_0l}{2P}\right)L + \frac{F_0l^2}{6P} - \frac{q_0}{Pk^2}. \tag{8}$$

Because the deflection curve is continuous and smooth, and there is the same angle and deflection in the gangue filling range C, the deflection is also the same. When $x = l$, we can obtain the following:

$$\begin{aligned}&A\cos kl + B\sin kl - \frac{F_0l^3}{6Pl} + \left(\frac{F_0}{2P} - \frac{q_0}{2P}\right)l^2 + \frac{R_Al}{P} \\ &\quad - \frac{F_0l}{Plk^2} + \frac{F_0 - q_0}{Pk^2} \\ &= C\cos kl + D\sin kl - \frac{q_0}{2P}l^2 + \left(\frac{R_A}{P} + \frac{F_0l}{2P}\right)l \\ &\quad - \frac{F_0l^2}{6P} + \frac{q_0}{Pk^2}.\end{aligned} \tag{9}$$

Therefore, we can also obtain the following:

$$\begin{aligned}&-Ak\sin kl + Bk\cos kl - \frac{F_0l}{2P} + \frac{F_0l}{P} - \frac{q_0l}{P} + \frac{R_A}{P} - \frac{F_0}{Plk^2} \\ &= -Ck\sin kl + Dk\cos kl - \frac{q_0l}{P} + \frac{R_A}{P} + \frac{F_0l}{2P}.\end{aligned} \tag{10}$$

Set $G = q_0/2PL^2 - (R_A/P + F_0l/2P)L + (F_0l/6P) - (q_0/Pk^2)$. The simultaneous formula can be obtained as follows:

$$\begin{cases} A = \dfrac{F_0 - q_0}{Pk^2}, \\ B = \dfrac{F_0 - q_0}{Pk^2}\tan kl - \dfrac{G\tan kl}{\cos kL} + \dfrac{F_0}{Plk^3\cos kl} + \dfrac{1}{\tan^2 kl - 1}\left(\tan kl + \dfrac{1}{\tan kL}\right) \\ \quad \cdot\left[-\dfrac{F_0 - q_0}{Pk^2}\left(1 + \tan^2 kl\right) + \dfrac{G\left(\tan^2 kl + 1\right)}{\cos kL} - \dfrac{F_0\tan kl}{Plk^3\cos kl} + \dfrac{2q_0}{Pk^2\cos kl}\right], \\ C = \dfrac{G}{\cos kL} - \left(\dfrac{1}{\tan^2 kl - 1}\right)\left[-\dfrac{F_0 - q_0}{Pk^2}\left(1 + \tan^2 kl\right) + \dfrac{G\left(\tan^2 kl + 1\right)}{\cos kL} - \dfrac{F_0\tan kl}{Plk^3\cos kl} + \dfrac{2q_0}{Pk^2\cos kl}\right], \\ D = \dfrac{1}{\tan kL\left(\tan^2 kl - 1\right)}\left[-\dfrac{F_0 - q_0}{Pk^2}\left(1 + \tan^2 kl\right) + \dfrac{G\left(\tan^2 kl + 1\right)}{\cos kL} - \dfrac{F_0\tan kl}{Plk^3\cos kl} + \dfrac{2q_0}{Pk^2\cos kl}\right]. \end{cases} \tag{11}$$

Four constants in the deflection curve equation are solved. Due to the limited subsidence of the roof in the gangue sliding and filling area, the maximum deflection is in the range of $l \le x \le L$; that is,

$$\begin{aligned}\omega &= C\cos kx + D\sin kx - \frac{q_0}{2P}x^2 + \left(\frac{R_A}{P} + \frac{F_0l}{2P}\right)x \\ &\quad - \frac{F_0l^2}{6P} + \frac{q_0}{Pk^2}, \quad (l \le x \le L).\end{aligned} \tag{12}$$

When $d\omega/dx = 0$, there is a maximum value:

$$\frac{d\omega}{dx} = -Ck\sin kx + Dk\cos kx - \frac{q_0x}{P} + \frac{R_A}{P} + \frac{F_0l}{2P} = 0. \tag{13}$$

However, it is difficult to solve the previously mentioned equation, so the principle of minimum potential energy is used to solve the displacement. In general, we can select the components of displacement as

$$u = u_0(x, y, z) + \sum_m A_m u_m(x, y, z),$$
$$v = v_0(x, y, z) + \sum_m B_m v_m(x, y, z), \quad (14)$$
$$w = w_0(x, y, z) + \sum_m C_m w_m(x, y, z).$$

For the bending deformation of rock beam, we only need to consider the deformation of one component., i.e.,

$$\omega = \omega_0(x) + \sum_m C_m \omega_m(x). \quad (15)$$

According to the roof stress of coal seam, the boundary conditions are as follows:

$$\omega(0) = \omega(L) = 0,$$
$$\omega'(0) = \omega'(L) = 0. \quad (16)$$

One of the solutions satisfying the previously mentioned boundary conditions is

$$\omega = \sum_m C_m x^{m+1}(1 - x). \quad (17)$$

In order to find the approximate solution of the above function, take one of the following terms:

$$\omega = C_1 x^2 (1 - x). \quad (18)$$

The bending strain energy of rock beam is

$$U = \frac{\mathrm{EI}}{2} \int_0^L \left(\frac{\mathrm{d}^2\omega}{\mathrm{d}x^2}\right)^2 \mathrm{d}x. \quad (19)$$

Substituting (18) into the formula, we can obtain the following:

$$U = 2\mathrm{EI}C_1^2 L^3. \quad (20)$$

Next, calculate the work done by the external force, and the work done by the gravity $q0$ of the overburden is as follows:

$$w_1 = \int_0^l q_0 C_1 x^2 (L - x)\mathrm{d}x = \frac{1}{12} C_1 q_0 L^4. \quad (21)$$

The work done by the filling supporting force of the collapsed gangue is as follows:

$$w_2 = \int_0^l q_1 C_1 x^2 (L - x)\mathrm{d}x = C_1 q_1 l^3 \left(\frac{L}{3} - \frac{l}{4}\right). \quad (22)$$

The work done by the axial force P is as follows:

$$w_3 = \int_0^L P \frac{(\omega')^2}{2} \mathrm{d}x = \frac{1}{15} P C_1^2 L^5. \quad (23)$$

According to the energy balance theorem, the work done by all forces and the internal energy change are equal, i.e.,

$$U = w_1 + w_2 + w_3. \quad (24)$$

After substituting into the equation, the solution is as follows:

$$C_1 = \frac{(1/12)q_0 L^4 + q_1 l^3 ((L/3) - (L/3))}{2\mathrm{EIL}^3 - (1/15)\left(\mathrm{PL}^5\right)}. \quad (25)$$

By substituting the equation (25) into the deflection equation, we can obtain the following:

$$\omega = \frac{(1/12)q_0 L^4 + q_1 l^3 (L/3 - L/4)}{2\mathrm{EI}L^3 - (1/15)\mathrm{PL}^5}. \quad (26)$$

In the mining of steep coal seam, the maximum deflection is in the range of $l \le x \le L$, and in this range $q1 = 0$, i.e.,

$$\omega = \frac{(1/12)q_0 L^4}{2\mathrm{EI}L^3 - (1/15)\mathrm{PL}^5} x^2 (L - x) = \frac{(1/12)q_0 L^4}{2\mathrm{EI} - (1/15)\mathrm{PL}^5} x^2 (L - x). \quad (27)$$

The deflection equation is derived on the whole working face (L) $\mathrm{d}\omega = \mathrm{d}x$, and the position of the largest deflection can be obtained, $(2/3)L$, so we can conclude that the maximum deflection of the roof occurs in the middle and upper part of the goaf.

4. Similar Simulation Experiment

4.1. Coal Mine Parameters. Based on the engineering background of #2463 working face of Xiangyong coal mine, the deformation and failure law of overlying strata after mining steep coal seam is simulated. Coal seam #6 is the main coal seam of the mine, with a thickness of 0.5–28.3 m and an average of 1.75 m. The roof is siltstone or medium-fine-grained sandstone, and the bottom plate is fine sandstone or siltstone. The structure of the coal seam is relatively simple, including some gangue layers. The coal seam has a strike of about 30°, a tendency of 120°, a dip angle of 5° to 85°, and an average dip angle of 60°, which belongs to the steeply inclined coal seam. The average mining depth is 550 m, and the average inclined length of the working face is 100 m, advancing along the strike. The detailed mechanical parameters of each stratum are demonstrated in Table 1.

4.2. Parameters and Making of Similar Model. In the similarity simulation experiment, the horizontal type multiangle plane similarity simulation experimental device developed by ourselves was used to carry out the plane strain model experiment [32]. The size of the model is 2.5 m × 0.2 m × 2 m, and the upper part was loaded with gravity compensation stress. The similarity simulation test bench is show in Figure 2.

The similarity ratio constants of the models used in the experiment are shown in Table 2, and the mechanical parameters of each rock layer of the model are further determined by the similarity ratio constant and the mechanical parameters of each rock layer of the prototype. The whole experimental model is made of similar materials which are composed of river sand as aggregate and cement and gypsum as cementing material, and mica powder is used to separate the layers between the strata. The proportioning parameters of similar materials are demonstrated in Table 3.

Table 1: Mechanical parameters of surrounding rock.

Lithology	Δ (m)	P (kg.m^{-3})	E (GPa)	σ_c (MPa)	σ_t (MPa)	C (MPa)	υ	φ (°)
Siltstone	58.36	2590	19.5	56.26	1.84	55	0.21	37
Medium sandstone	40.4	2600	13.5	36.42	1.13	16	0.12	38
Siltstone	21.04	2590	19.5	56.26	1.84	55	0.21	37
Sandy mudstone	5.74	2150	5.4	28.65	0.75	45	0.18	31
Coal seam #6	1.75	1450	5.1	14	0.45	1.35	0.36	24
Medium sandstone	13.8	2800	14.2	36.42	1.13	16	0.12	38
Sandy mudstone	35.06	2150	5.4	28.65	0.75	45	0.18	31
Siltstone	27.65	2590	19.5	56.26	1.84	55	0.21	37

Figure 2: Similarity simulation test bench.

Table 2: Similar ratio of model.

Similar constants	Geometric (α_l)	Unit weight (α_l)	Time (α_t)	Dynamics (R_M)
Similarity ratio	1 : 100	0.7 : 1	0.05	$0.007 \times R_H$(prototype)

Table 3: The proportioning parameters of similar materials.

Num	Lithology	Materials	Ratio (aggregate: cementing material)	Ratio (gypsum: cement)
1	Siltstone	Sand: gypsum: cement	8.5 : 1.5	9 : 1
2	Medium sandstone	Sand: gypsum: cement	7.5 : 5	8.5 : 1.5
3	Siltstone	Sand: gypsum: cement	8.5 : 1.5	9.5 : 0.5
4	Sandy mudstone	Sand: gypsum: cement	8.5 : 1.5	9 : 1
5	Coal seam #6		Coal is mixed with water and compacted	
6	Medium sandstone	Sand: gypsum: cement	7.5 : 5	8.5 : 1.5
7	Sandy mudstone	Sand: gypsum: cement	8.5 : 1.5	9 : 1
8	Siltstone	Sand: gypsum: cement	8 : 2	8.5 : 1.5

4.3. Monitoring of Model. In this paper, the physical similarity simulation experiment is used to explore the failure law of overburden in a fully mechanized mining face of the steep coal seam. It is necessary to make a series of observations on the deformation and failure of some rock strata and the stress change inside the rock strata in this experiment. According to the characteristics of strata failure and movement in steeply inclined coal seam mining, two lines of horizontal monitoring lines are arranged at the upper part of the model to simulate the surface subsidence displacement, and the distance between the monitoring points is 10 cm. Six displacement monitoring lines are arranged on the roof along the layer direction of the coal seam, the horizontal spacing of the monitoring points is 5 cm, and the inclined spacing is 10 cm. Two displacement monitoring lines are arranged on the floor, with a horizontal spacing of 5 cm and an inclined spacing of 10 cm. The layout of the monitoring points is shown in Figure 3. The red frame is the total station of the displacement monitoring instrument. The total station used in this paper is Kolida KTS-442RC prism-free infrared total laser station; single prism range: 5000m; prism-free range: 350m; ranging accuracy: 2 + 2 ppm; angle measurement accuracy: 2″.

5. Analysis of Similar Simulation Experiment Results

5.1. Analysis of Displacement Results

5.1.1. Analysis of Displacement Change of Roof in Goaf. Simulated mining was carried out on the model according to the time calculated by the time similarity ratio, displacement

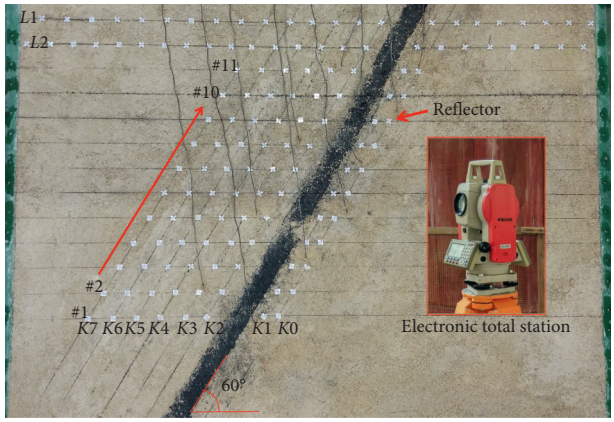

Figure 3: Model arrangement of monitoring points.

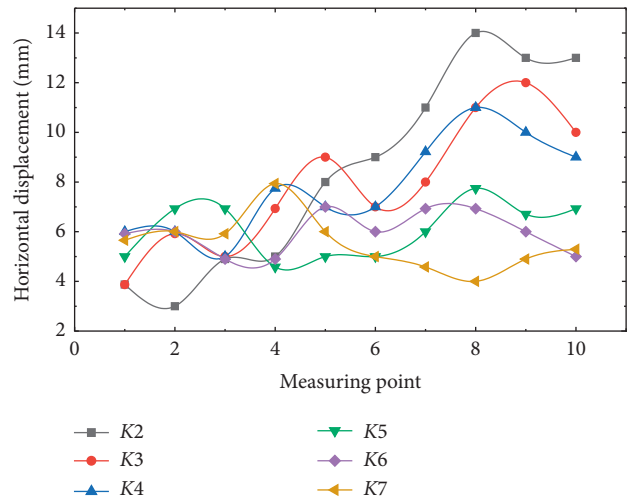

Figure 4: Horizontal displacement changes of roof monitoring points.

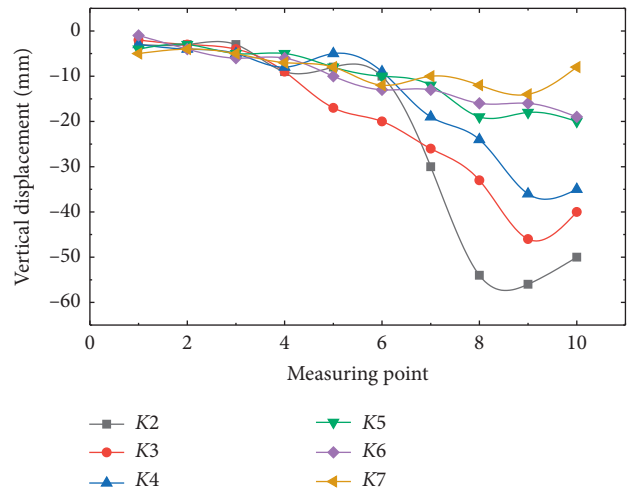

Figure 5: Vertical displacement changes of roof monitoring points.

monitoring was carried out, and a small amount of invalid monitoring data was removed. The horizontal displacement change diagram of $K2 \sim K7$ monitoring line of the roof after coal mining is shown in Figure 4. It can be seen from Figure 4 that the horizontal displacement changes of the upper roof of the goaf are greater than the horizontal displacement of the lower roof of the goaf, which shows that, in the mining process of the steep coal seam, the deformation and damage mainly occur in the upper part of the goaf. At the same time, the immediate roof naturally falls to the lower part of the goaf, which plays a supporting role in the lower roof of the goaf, thus limiting the deformation and damage of the roof. The horizontal displacement of the roof monitoring point in the lower part of the goaf is 3–8.2 mm, with an average of 5.9 mm. The maximum horizontal displacement on the roof monitoring line is 13.9 mm.

The vertical displacement change diagram of $K_2 \sim K_7$ monitoring line of the roof after coal mining is shown in Figure 5. There is a significant difference between the vertical displacement of the upper roof and the lower roof of the goaf after coal mining, and large deformation and collapse occur in the upper roof, which indicates that the phenomenon of collapse occurs in the immediate roof in the middle and upper parts of the working face. The first position of collapse is also from the middle and upper parts of the working face. At the same time, after the immediate roof falls to the lower part of the goaf, it has a reasonable restriction on the roof in the vertical direction. The vertical displacement of the roof monitoring point at the lower part of the goaf is 1–10 mm, with an average of 7.4 mm. The maximum vertical displacement on the roof monitoring line is 57.5 mm.

5.1.2. Analysis of the Results of Displacement Change of Horizontal Monitoring Line. The displacement change diagram of the monitoring line L1-L2 of the experimental model simulating the surface subsidence is shown in Figure 6. It can be seen from the figure that the displacement of the rock strata directly above the goaf in the horizontal direction is relatively small, and there is only a large fluctuation in the vertical direction of the goaf in the working face, and the deformation has also moved left to right tendency. The deformation of the horizontal monitoring line is massive in the vertical direction, especially the area directly above the goaf, which reaches the maximum, and the vertical displacement of the monitoring point reaches a maximum of 25 mm.

Based on the analysis of the previously mentioned monitoring results, the deformation of the roof in the goaf mainly occurs in the upper and middle parts. The lower roof automatically falls to the lower part of the goaf due to the immediate roof collapse, which plays a particular supporting role in the lower roof and makes the deformation of the lower roof generally smaller. The strata directly above the goaf are deformed in the vertical direction, so the area and range of surface subsidence can be inferred.

5.2. Analysis of Movement and Failure Law of Overburden. The rock strata movement and failure form of a similar model after mining is shown in Figure 7. As shown in the

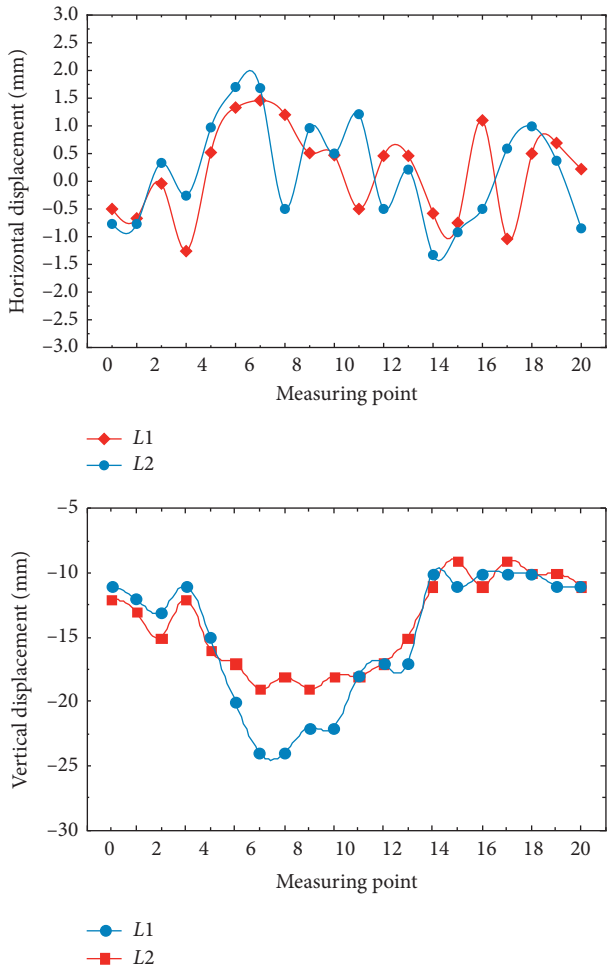

Figure 6: Near-ground surveillance line water level transition.

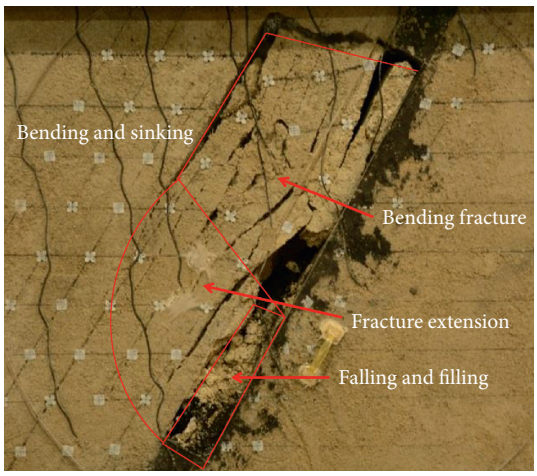

Figure 7: Collapse form diagram.

figure, the overburden of the working face has a large area of collapse, forming a unique collapse failure pattern and law of steep coal seam mining. Due to the large inclination of the coal seam, the immediate roof gangue automatically slides down to the lower goaf and supports the lower roof, and only

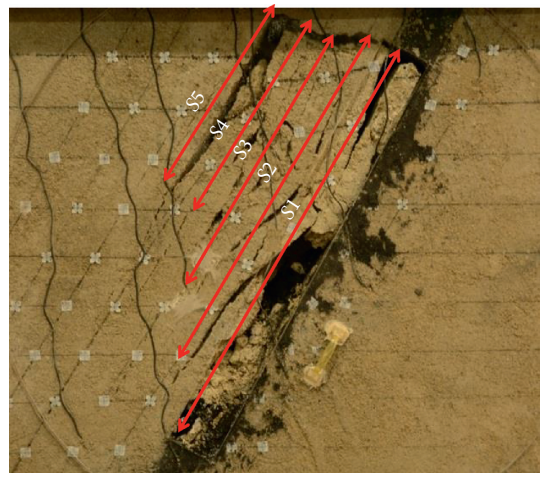

Figure 8: Fracture analysis diagram.

a small amount of sinking occurs in the lower roof. The upper part of the goaf is exposed in a large area and the roof is broken and comes in contact with the floor, forming a hinged structure in a small area and reaching a state of balance. The roof fracture in the upper part of the working face forms a "trapezoid" bending fracture area as shown in Figure 7, in which the upper part of the dip rock beam is a direct tensile fracture and the interlayer rock layer is a beam fracture. The fracture line is located in the middle and upper parts of the working face. The whole overlying strata have formed a secondary stability system, which is composed of four areas: the lower falling and filling support area, the upper strata bending fracture area, the fracture extension area, and the roof bending sinking area. At the same time, the fracture line of the goaf roof is located in the middle and upper parts of the working face, which is consistent with the results derived from the mechanical model. The overlying strata began to break at the position with the maximum deflection, and the fracture position gradually moved up due to the collapse and filling of the lower part, and the fracture line was basically in the middle of the "trapezoidal" bending fracture area.

As shown in Figure 8, the roof is simplified as inclined rock beam, and the roof is exposed after mining; the roof will break when the length of the exposed rock beam is greater than the limit span of the inclined rock beam. The hanging length of the roof is simplified as $S1 \sim S5$. It can be seen that the hanging area of the roof is gradually reduced due to the supporting effect of the immediate roof caving gangue sliding to the lower goaf on the lower roof, but $S2$, $S3$, and $S4$ are still more massive than the limit span of the rock stratum, and the roof is still broken. Besides, the fracture position of the roof gradually moves upward. Under the influence of the filling of the natural falling gangue in the lower part, the hanging length of the upper roof decreases from one layer to another until the hanging length is less than the limit span of the rock stratum. In Figure 8, $S5$ will not break any more, only a small amount of cracks are produced between the strata, and the only displacement has occurred towards the direction of the goaf. The displacement of the roof above the

"trapezoid" bending fracture area still occurs. However, the fracture does not occur because the hanging area of the rock stratum is reduced, and the limit span of the rock stratum is not exceeded.

6. Conclusions

(1) In this paper, the mechanical model of the roof after the mining of steep coal seam is established, the basic roof is simplified as the mechanical model of inclined rock beam, and the bending deflection equation of the roof rock beam is analyzed. The derivation of the deflection equation shows that the maximum deflection position of the roof rock beam appears at $2/3l$, i.e., the middle and upper parts of the goaf.

(2) The roof deformation of the goaf is more extensive after the working face has been pushed along the strike, and the deformation mainly occurs in the upper roof of the goaf. The collapse phenomenon occurs in the immediate roof, and the gangue behind the collapse fills the lower part of the goaf, which plays a supporting and restricting role in the lower roof of the goaf. At the same time, it can be inferred that the surface subsidence is concentrated above the goaf.

(3) After the upper roof of the goaf in the steep coal seam is broken, a "trapezoidal" bending fracture zone is formed, and the lower roof is in the form of interlayer fracture. The secondary stability system is formed, which is composed of four areas: the lower falling and filling support area, the upper strata bending fracture area, the fracture extension area, and the roof bending sinking area.

(4) The position of roof fracture line in goaf of the steep coal seam is located in the middle and upper part of the working face, which is consistent with the results derived from the mechanical model. The overlying strata begin to break at the maximum deflection position, and the fracture position gradually moves up due to the collapse and filling of the lower part.

Data Availability

The data used to support the findings of this study are available from the corresponding author upon request.

Conflicts of Interest

The authors declare that they have no conflicts of interest.

Acknowledgments

The authors would like to acknowledge the support and contribution from the School of Resources, Environment and Safety Engineering, Hunan University of Science and Technology, China. This research was funded by the National Natural Science Foundation of China (51274095 and 51974117) and the Natural Science Foundation of Hunan Province (2020JJ4027).

References

[1] G. Wu, W. Chen, S. Jia et al., "Deformation characteristics of a roadway in steeply inclined formations and its improved support," *International Journal of Rock Mechanics and Mining Sciences*, vol. 130, Article ID 104324, 2020.

[2] X. Li, Z. Wang, and J. Zhang, "Stability of roof structure and its control in steeply inclined coal seams," *International Journal of Mining Science and Technology*, vol. 27, no. 2, pp. 359–364, 2017.

[3] J.-P. Zuo, J.-H. Wen, Y.-D. Li et al., "Investigation on the interaction mechanism and failure behavior between bolt and rock-like mass," *Tunnelling and Underground Space Technology*, vol. 93, Article ID 103070, 2019.

[4] Y. Sun, J. Zuo, M. Karakus, and J. Wen, "A novel method for predicting movement and damage of overburden caused by shallow coal mining," *Rock Mechanics and Rock Engineering*, vol. 53, no. 4, pp. 1545–1563, 2020.

[5] J. Zuo, J. Wang, and Y. Jiang, "Macro/meso failure behavior of surrounding rock in deep roadway and its control Technology," *International Journal of Coal Science & Technology*, vol. 6, no. 3, pp. 301–319, 2019.

[6] G. S. Wu, W. J. Yu, J. P. Zuo, C. Y. Li, J. H. Li, and S. H. Du, "Experimental investigation on rockburst behavior of the rock-coal-bolt specimen under different stress conditions," *Scientific Reports*, vol. 10, no. 1, 2020.

[7] G. Wu, W. Yu, Z. Liu, and Z. Tang, "Failure law and mechanism of the rock-loose coal composite specimen under combined loading rate," *Advances in Civil Engineering*, vol. 2018, Article ID 2482903, 10 pages, 2018.

[8] W. Yu, B. Pan, F. Zhang, S. Yao, and F. Liu, "Deformation characteristics and determination of Optimum supporting time of alteration rock mass in deep mine," *KSCE Journal of Civil Engineering*, vol. 23, no. 11, pp. 4921–4932, 2019.

[9] F. Gong, J. Yan, X. Li, and S. Luo, "A peak-strength strain energy storage index for rock burst proneness of rock materials," *International Journal of Rock Mechanics and Mining Sciences*, vol. 117, pp. 76–89, 2019.

[10] X. Si and F. Gong, "Strength-weakening effect and shear-tension failure mode transformation mechanism of rockburst for fine-grained granite under triaxial unloading compression," *International Journal of Rock Mechanics and Mining Sciences*, vol. 131, Article ID 104347, 2020.

[11] F.-Q. Gong, Y. Luo, X.-B. Li, X.-F. Si, and M. Tao, "Experimental simulation investigation on rockburst induced by spalling failure in deep circular tunnels," *Tunnelling and Underground Space Technology*, vol. 81, pp. 413–427, 2018.

[12] Y. P. Wu, "Dymamic model and stability of system "roof-support-floor" in steeply dipping seam mining," *Jouranl of China Coal Society*, vol. 05, pp. 527–531, 2004.

[13] F. Yang, *Study on Overburden Strata'S Movement Pattern and Mechanism of Mining Steeply Inclined Seams*, Liaoning Technical University, Fuxin, China, 2006.

[14] Y. D. Zhang, J. Y. Cheng, and X. X. Wang, "Thin plate model analysis on roof break of up-dip or down-dip mining stope," *Journal of Mining and Safety Engineering*, vol. 27, no. 4, pp. 487–493, 2010.

[15] H.-S. Tu, S.-H. Tu, D.-F. Zhu, D.-Y. Hao, and K.-J. Miao, "Force-fracture characteristics of the roof above goaf in a steep coal seam: a case study of xintie coal mine," *Geofluids*, vol. 2019, Article ID 7639159, 11 pages, 2019.

[16] H. Tu, S. Tu, Y. Yuan, F. Wang, and Q. Bai, "Present situation of fully mechanized mining Technology for steeply inclined

coal seams in China," *Arabian Journal of Geosciences*, vol. 8, no. 7, pp. 4485–4494, 2015.

[17] H. S. Tu, S. H. Tu, F. Chen, C. Wang, and Y. F. Feng, "Study on the deformation and fracture feature of steep inclined coal seam roof based on the theory of thin plates," *Journal of Mining and Safety Engineering*, vol. 31, no. 1, pp. 49–54, 2014.

[18] J. Lu, G. Yin, H. Gao et al., "True triaxial experimental study of disturbed compound dynamic disaster in deep underground coal mine," *Rock Mechanics and Rock Engineering*, vol. 53, no. 5, pp. 2347–2364, 2020.

[19] G. Z. Yin, D. K. Wang, and W. Z. Zhang, "Mechanics model to deformation of covered rock stata and its application in deep mining of steep or inclined seam," *Journal of Chongqing University (Natural Science Edition)*, vol. 2, pp. 79–82, 2006.

[20] P. S. Xie, Y. P. Wu, S. H. Luo, H. W. Wang, and D. Lang, "Structural evolution of ladder roof and its stability analyses for a fully-mechanized working face with a large mining height in steeply inclined coal seam," *Journal of Mining and Safety Engineering*, vol. 35, no. 5, pp. 953–959, 2018.

[21] P. S. Xie, Y. P. Wu, H. W. Wang, and S. G. Ren, "Interaction characteristics between strata movement and support system Around large mining height fully-mechanized face in steeply inclined seam," *Journal of Mining and Safety Engineering*, vol. 32, no. 1, pp. 14–19, 2015.

[22] P. S. Xie, Y. P. Wu, and H. W. Wang, "Stability analysis of incline masnry structure and support around longwall mining face area in steeply dipping seam," *Jouranl of China Coal Society*, vol. 37, no. 8, pp. 1275–1280, 2012.

[23] H. W. Wang, Y. P. Wu, and P. S. Xie, "Formation and evolution characteristics of rock stress field in steeply dipping seam mining," *Journal of Liaoning Technical University(Natural Science)*, vol. 32, no. 8, pp. 1022–1026, 2013.

[24] Q. Yao, T. Feng, and Z. Liao, "Damage characteristics and movement of inclined strata with sublevel filling along the strike in the steep seam," *Jouranl of China Coal Society*, vol. 42, no. 12, pp. 3096–3105, 2017.

[25] Q. Yao, T. Feng, Z. Liao, and C. F. MA, "Stress distribution of the roof initial fracture feature for sublevel fill mining along the strike in steep coal seam," *Journal of Mining and Safety Engineering*, vol. 34, no. 6, pp. 1148–1155, 2017.

[26] X.-P. Lai, M.-F. Cai, F.-H. Ren, P.-F. Shan, F. Cui, and J.-T. Cao, "Study on dynamic disaster in steeply deep rock mass condition in urumchi coalfield," *Shock and Vibration*, vol. 2015, Article ID 465017, 8 pages, 2015.

[27] H. Alehossein and B. A. Poulsen, "Stress analysis of longwall top coal caving," *International Journal of Rock Mechanics and Mining Sciences*, vol. 47, no. 1, pp. 30–41, 2010.

[28] S. Karekal, R. Das, L. Mosse, and P. W. Cleary, "Application of a mesh-free continuum method for simulation of rock caving processes," *International Journal of Rock Mechanics and Mining Sciences*, vol. 48, no. 5, pp. 703–711, 2011.

[29] J. A. Wang and J. L. Jiao, "Criteria of support stability in mining of steeply inclined thick coal seam," *International Journal of Rock Mechanics and Mining Sciences*, vol. 82, pp. 22–35, 2016.

[30] Z. Yuan, Y. Shao, and Z. Zhu, "Similar material simulation study on protection effect of steeply inclined upper protective layer mining with varying interlayer distances," *Advances in Civil Engineering*, vol. 2019, Article ID 9849635, 14 pages, 2019.

[31] S. He, D. Song, X. He et al., "Coupled mechanism of compression and prying-induced rock burst in steeply inclined coal seams and principles for its prevention," *Tunnelling and Underground Space Technology*, vol. 98, p. 103327, 2020.

[32] Z. Liao, T. Feng, Q. Yao, and C. F. Ma, "Development of plane similar simulation experiment device for steep seam mining," *Mineral Engineering Research*, vol. 33, no. 2, pp. 18–22, 2018.